

Skilful probabilistic predictions of UK flood risk months ahead using a large-sample machine learning model trained on multimodel ensemble climate forecasts

Simon Moulds^{1,2*}, Louise Slater², Louise Arnal³, Andy Wood^{4,5}

¹ School of GeoSciences, University of Edinburgh, UK [@simmoulds].

² School of Geography and the Environment, University of Oxford, UK.

³ Ouranos, Montreal, Canada

⁴ Climate and Global Dynamics, National Center for Atmospheric Research, Boulder, CO, USA

⁵ Department of Civil and Environmental Engineering, Colorado School of Mines, Golden, CO, USA

* Corresponding author email: simon.moulds@ed.ac.uk

This EarthArXiv original preprint is under review at Hydrology and Earth System Science (HESS).

Abstract

Seasonal streamflow forecasts are an important component of flood risk management. Hybrid forecasting methods that predict seasonal streamflow using machine learning models driven by climate model outputs are currently underexplored, yet have some important advantages over traditional approaches using hydrological models. Here we develop a hybrid subseasonal to seasonal streamflow forecasting system to predict the monthly maximum daily streamflow up to four months ahead. We train a quantile regression forest model on dynamical precipitation and temperature forecasts from a multimodel ensemble of 196 members (eight seasonal climate forecast models) from the Copernicus Climate Change Service (C3S) to produce probabilistic hindcasts for 579 stations across the UK for the period 2004-2016, with up to four months lead time. We show that the large-sample (multi-site) ML model trained on pooled catchment data together with static catchment attributes is narrowly but significantly more skilful compared to single-site ML models trained on data from each catchment individually. Considering all initialization months, 60% of stations show positive skill ($\text{CRPSS} > 0$) relative to climatological reference forecasts in the first month after initialization. This falls to 41% in the second month, 38% in the third month and 33% in the fourth month.

1 Introduction

Reliable streamflow forecasts weeks to months ahead are vital for managing the impacts of hydrological variability and extremes. Dynamical subseasonal to seasonal (S2S) streamflow forecasts are commonly produced by forcing a conceptual or physics-based hydrological model with the outputs of dynamical seasonal forecasts from climate models, and may also include a subsequent statistical or machine learning post-processing step. This may be achieved either directly or indirectly – e.g., by using dynamical climate prediction information as direct inputs to the hydrological model, or by using the dynamic predictions or empirical information as conditioning factors in a statistical weather generation scheme to create the model's input meteorological forecasts. These systems represent the current standard in S2S streamflow forecasting, underpinning flood forecasting services in Europe (Arheimer et al., 2020; Arnal et al., 2018), the USA (Demargne et al., 2014), Australia (Bennett et al., 2017), and globally (Emerton et al., 2018).

The chaotic nature of the atmosphere places a time limit of around 14 days on the predictability of weather from initial atmospheric circulation conditions, although this limit may vary from less than a week to nearly three weeks depending on local climate features and the current weather regime. S2S hydro-meteorological forecasts therefore rely on relatively slowly-varying aspects of the climate system that are more predictable beyond weather time scales, including initial hydro-meteorological conditions and large-scale climate variability modes (Doblas-Reyes et al., 2013; Emerton et al., 2018). While the skill of seasonal climate forecasts is relatively low in the extra-tropics compared to other parts of the world (Doblas-Reyes et al., 2013), recent progress in forecasting European climate has resulted in skilful seasonal climate forecasts that support various climate services (e.g. Arheimer et al., 2020). For example, the European Flood Awareness System (EFAS) is at the forefront of operational streamflow forecasting in Europe, providing a pan-European service that aims to support preparatory action before major floods. The seasonal component of EFAS uses precipitation, temperature and evaporation from the ECMWF System 5 (SEAS5) seasonal prediction system to drive LISFLOOD, a physics-based distributed hydrological model that estimates hydrological states and fluxes with a daily time step (Arnal et al., 2018). Operationally, EFAS produces seasonal streamflow outlooks for Europe at the beginning of each month up to seven months ahead. Previous work using this setup suggests that skilful forecasts may be obtained for lead times up to one month ahead, but that skill decreases gradually thereafter (Arnal et al., 2018).

The conceptual and physics-based hydrological models used operationally are computationally intensive relative to data-driven (statistical, empirical, machine learning) approaches. Spatial downscaling and bias correction of meteorological forecasts are needed to bridge the gap between the relatively coarse spatial scale of S2S climate prediction systems and the finer resolution inputs needed by hydrological models, introducing a layer of methodological uncertainty to the process-based seasonal hydrologic forecasting process. The hydrological forecast outputs may then require further bias-correction before they can be used (Yuan et al., 2015). In contrast, hybrid methods for seasonal streamflow forecasting overcome many of the shortcomings of dynamical approaches (Slater et al. 2023). Instead of using the downscaled outputs of dynamical seasonal prediction systems to drive a hydrological model, hybrid methods use dynamical climate predictions to drive statistical or

machine-learning models to directly predict the target variables of interest – e.g. streamflow quantiles or flood frequency. The dynamical climate predictions provide valuable information on large-scale climate patterns and atmospheric conditions, while the statistical or machine-learning models offer the ability to capture complex nonlinear relationships related to streamflow behaviour. Such hybrid approaches follow from similar concepts used in empirical S2S hydrologic prediction, in which observed climate system variables, reanalyses or indices (but not dynamical climate forecasts) are used in statistical schemes to predict streamflow directly (e.g. Mendoza et al., 2017; Regonda et al., 2006).

By combining the strengths of both dynamical and statistical approaches, hybrid methods have shown promise for improving seasonal streamflow predictions. For example, Tian et al. (2022) developed a hybrid framework that skilfully predicted month-ahead reservoir inflows in two US watersheds (in Colorado and Alabama) using an ML model driven by seasonal climate forecasts, observed large-scale climate indices and satellite-based estimates of antecedent conditions. In Europe, Hauswirth et al. (2023) showed that a single-site hybrid seasonal forecasting system could skilfully predict surface water level up to three months ahead using ML models driven by climate and hydrological inputs from SEAS5. Hybrid methods are unconstrained by the need to conserve the water balance and can implicitly handle biases in the climate data (Slater et al., 2023). Further, they are able to exploit relationships between variables at different spatial and temporal resolutions and spatial extents – e.g. relating daily local streamflow quantiles to monthly climate inputs or large-scale climate patterns (Moulds et al., 2023; Tian et al., 2022).

Previous work using observed data for hydrological simulation has shown that ML models work best when trained on data from multiple catchments (Nearing et al., 2021). While much of the recent literature on this topic focuses on deep learning architectures (e.g. Kratzert et al., 2019), similar results have been found for tree-based models (e.g. Gauch et al., 2021). Large-sample (or multi-site) approaches allow the models to learn relationships from a large envelope of hydrological variability that encompasses a broad spectrum of catchment characteristics, which they can use effectively to make predictions in individual catchments (e.g. Lees et al., 2021; Lees et al., 2022). However, the potential added value of a large-sample approach has not yet been evaluated for seasonal flood prediction using ML models trained on climate forecasts. Addressing this gap is necessary because seasonal

climate forecasts are typically highly uncertain, at levels of skill near a minimal threshold of uncertainty. The sample size of available records for training hydrological forecast models is much smaller at sub-seasonal to seasonal scales than at short to medium range scales. Thus, new methods that pool forecasts over space as well as time may be a promising strategy to extract greater forecast signal from small-sample noise.

Here we develop and test a hybrid forecasting system to predict the monthly maximum daily flow values (Q_{\max}) at lead times of up to four months for 579 catchments in the UK. The maximum probable flow in each month is an indicator of flood risk, though it does not predict the exact timing or volume of a future flood event. We train a large-sample machine learning model to predict Q_{\max} using seasonal forecasts of precipitation and temperature from the Copernicus Climate Change (C3S) multimodel ensemble alongside antecedent conditions and catchment characteristics. We focus on the monthly maximum daily streamflow rather than other common S2S hydrologic predictands (such as monthly or seasonal average flow) because it serves as an indicator of future flood hazards at S2S lead times while also presenting a significant challenge, as individual flood events (timing and magnitude) cannot be skilfully predicted beyond weather time scales. We address two main research questions: (i) How skilfully can the monthly maximum daily flow be predicted several months ahead using uncorrected monthly dynamical climate forecasts and antecedent conditions? (ii) To what extent can the skill of S2S streamflow predictions be improved at individual sites by developing a large-sample machine learning model that leverages static catchment attributes from a large collection of catchments to learn the hydrological behaviour at individual sites?

131 **2 Materials and methods**

132 **2.1 Data**

133 **2.1.1 Streamflow**

134 For the prediction target and observational validation dataset we used daily
135 streamflow observations for Great Britain from the National River Flow Archive (NRFA,
136 2024). We first selected stations that had streamflow records between 1994 and 2016 to
137 match the hindcast period of the climate models, before discarding stations with less than
138 95% data availability in any given year. We also discarded any stations that were not
139 included in the CAMELS-GB dataset (Coxon et al., 2020), leaving a total of 579 stations. We
140 computed specific discharge (mm day^{-1}) by dividing the daily streamflow values by the
141 catchment area, then calculated the monthly maximum daily specific discharge for all
142 months and stations.

143 **2.1.2 Climate (re)forecasts**

144 Monthly predictions of precipitation and temperature were obtained from the
145 Copernicus Climate Change (C3S) multimodel seasonal forecasting system. We took
146 seasonal reforecasts (“hindcasts”) of precipitation and temperature for the period 1994-
147 2016 from eight seasonal prediction systems, resulting in a large multimodel ensemble of
148 196 members (Table S1). We computed the multimodel ensemble mean values of
149 precipitation and temperature. We found that including quantiles (0.05, 0.25, 0.5, 0.75,
150 0.95) drawn from the precipitation and temperature ensemble as additional covariates
151 alongside the mean values in the ML models did not improve skill (results not shown). We
152 computed the climate inputs for each catchment by taking the area-weighted average
153 monthly value for each variable. All C3S forecasting systems are assigned a nominal start
154 date of the first day of each month such that no members are initialized using observations
155 later than this date, although the initialization method varies across the individual systems.
156 Hereafter we refer to the predictions for the month immediately following initialization as
157 having a lead time of zero (e.g. for a forecast initialized on August 1st, the zeroth lead time
158 prediction covers August 1-31st). The C3S forecasting system predicts climate up to a
159 minimum of 6 months ahead, but we focus on the first 4 months following initialization as

we are unlikely to observe substantial skill for monthly predictands thereafter (e.g. Arnal et al., 2018; Harrigan et al., 2018).

2.1.3 Antecedent catchment conditions

We used antecedent mean monthly streamflow as a proxy indicator of initial catchment soil moisture conditions, an important driver of seasonal hydrologic predictability (Arnal et al., 2018; Bierkens & Van Beek, 2009). We used the monthly mean specific discharge in the three months prior to the forecast initialization to create three predictor variables describing the mean specific discharge over one month, two months and three months prior to the nominal forecast initialization date, respectively. We also included estimates of antecedent precipitation using ERA5 reanalysis data, creating variables to represent the average precipitation over one month, two months and three months prior to the initialization time. Antecedent precipitation and streamflow are both employed as proxies for hydrologic initial conditions and are likely to exhibit some degree of collinearity. However, as random forests are relatively robust to multicollinearity, we chose to retain both predictors in the model.

2.1.4 Catchment attributes

Large-sample ML models trained on data from hundreds of stream gauges simultaneously can benefit from additional information about spatial variability in catchment characteristics relative to single-site models (e.g. Lees et al., 2021, Slater et al., 2024). Here we included static catchment descriptors from the CAMELS-GB dataset (Table S3; Coxon et al., 2020) in our ML model. We also tried including streamflow signatures that describe the hydrologic behaviour of each catchment, including the baseflow index, slope of the flow duration curve, the 5th and 95th percentile of daily streamflow, and the mean daily streamflow. These were computed using data up to the start of the test period (2004) of our hybrid models, to prevent data leakage (i.e., the situation where a statistical or ML model is inadvertently trained on the same data it will later be tested on). However, although the signature predictors assumed high importance in the QRF model, they did not increase Q_{\max} forecasting skill, suggesting that the model can learn these hydrological characteristics from

the static catchment attributes alone. We therefore left out the streamflow signatures from the final multi-site model.

2.2 Methods

We predict the monthly maximum daily streamflow (Q_{\max}) using both dynamic and static predictor variables. Most large-sample ML approaches for hydrologic prediction employ Long Short Term Memory models (LSTMs), which are well-suited for sequential modelling at daily timesteps. However, in this study, we employ quantile regression forests (QRF; Meinshausen, 2006), a nonparametric ensemble method that is well-suited for working with single monthly aggregated forecasts from C3S. QRFs extend traditional random forests (Breiman, 2001) by estimating conditional quantiles of the response variable, enabling probabilistic predictions. Like random forests, QRFs are adept at exploiting nonlinear relationships between dependent and independent variables and require relatively little tuning because their performance is less sensitive to the values of hyperparameters compared to many other ML methods (Tyralis et al., 2019). QRFs can also be interrogated to establish the relative importance of predictor variables.

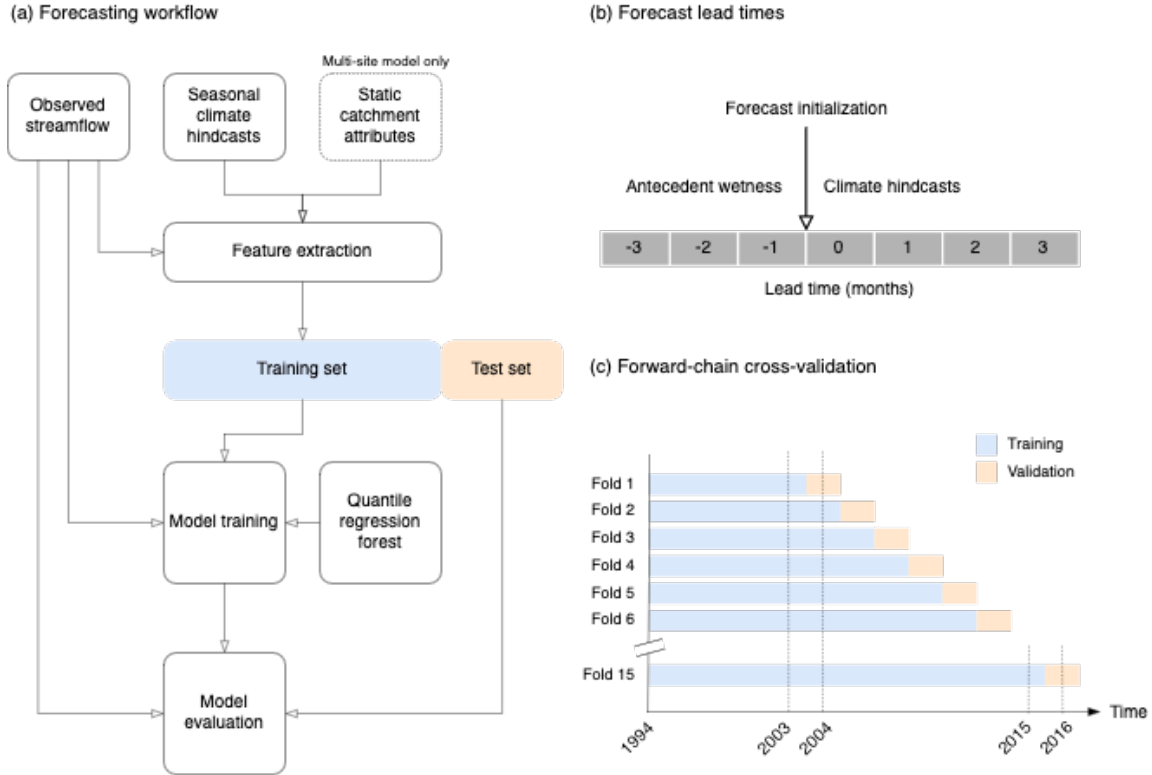


Figure 1: Key features of the forecast system. **a.** Overview of steps in the forecasting workflow. **b.** Forecast lead times used in the study. A separate model is trained for each lead time to account for changing climate model biases. **c.** Schematic of the forward-chain cross-validation procedure employed during model training.

2.2.1 Model training

We train the model directly on the dynamical S2S forecast outputs to avoid introducing additional uncertainty due to post-processing (Figure 1a). Like other forms of regression, the ML model implicitly performs bias correction by relating the raw climate inputs to observed streamflow (e.g. Slater et al. 2023; Slater and Villarini 2018). We compared three model structures to predict Q_{\max} in each catchment (Table 1). First, we trained QRF models on each streamflow time series independently, giving a site-specific model for every catchment. We compared the single-site models with a multi-site QRF model that was trained on all ($n=579$) available streamflow time series data at once. To assess the extent to which the multi-site model learns from catchment attributes, we also include a multi-site model with the catchment ID as the only static attribute. Owing to the inherent robustness of QRF to potentially irrelevant predictors, whereby unimportant

features are automatically downweighted, we do not perform predictor variable selection or screening.

Table 1: Formulation of the three ML models used in the analysis. Precipitation and temperature are the monthly ensemble mean values from the C3S multimodel system. Antecedent precipitation is the forecasted precipitation from the month prior to the target month, with lead time varying between 1 and 3 months (i.e. to make a prediction in lead time 4 the antecedent precipitation would be taken from lead time 3). Antecedent streamflow is the mean daily observed streamflow prior to the forecast initialization. Catchment attributes are listed in Table S1.

Model name	Configuration	Model description
<i>Single-site</i>	Single-site	Precipitation, temperature, antecedent streamflow and precipitation
<i>Multi-site with ID</i>	Multi-site	As for single-site model, plus catchment ID
<i>Multi-site with attributes</i>	Multi-site	As for single-site model, plus 15 static catchment attributes

In both single-site and multi-site approaches, a separate QRF model is trained for each lead time using all months from the training period. This is because the biases in the climate forecasts often change over time from initialization, so a model trained on climate forecasts with a lead time of one month would be unsuitable to make predictions using climate forecasts with a lead time of two months. We note that a similar approach is used for bias correcting seasonal climate forecasts (Crochemore et al., 2016). Another possibility would be to train a model on all lead times at once, with the lead time itself included as a categorical variable. We tried this but found that it degraded predictive skill. Thus, for each training period we obtain four models, trained on climate predictions with lead times of one, two, three and four months ahead, respectively (Figure 1b). Dataset stratification choices are important in S2S prediction because predictability and prediction system biases typically vary seasonally and with lead time. There are strong geophysical reasons to tailor a statistical or empirical model using both factors, but each stratification dimension reduces the sample size available for training and testing, thus a trade-off is often adopted (e.g. Lehner et al., 2017). Here we do not stratify by initialization date (i.e., month). We construct an ensemble forecast by using the QRF model to predict the conditional quantiles of Q_{\max} corresponding to probabilities between 0.01 and 0.99, with an interval of 0.02.

We use a forward-chain cross-validation approach whereby the models are trained on reforecasts from the previous n years and tested on the current year (Figure 1c). For example, to predict all months in 2004, the first training period was taken as January 1994 to December 2003. For 2005, we then extended the training period by one year to December 2004, and continued adding one year until 2016, the final year in the test period, at which point the training period for the QRF models was January 1994 to December 2015. The climate predictors consisted of the multimodel ensemble mean of monthly precipitation and temperature (Table S1). We did not include a separate validation dataset (i.e., in a train/validate/test framework) because we found there was limited benefit to be gained from tuning the hyperparameters of the QRF model. The forward-chain cross-validation approach means that the model was retrained each year using data up to the previous year. The overall test results combine the test results for the individual years. This ensures the model is never tested on data it has been exposed to during training.

2.2.2 Forecast evaluation

We evaluated predictive skill using the continuous ranked probability score (CRPS) and associated skill score (CRPSS), common metrics for ensemble forecast evaluation. The CRPS represents the error between the forecast and observed cumulative distribution functions (Wilks, 2019). It ranges between zero and positive infinity and is negatively oriented (i.e. smaller values are better), similar in concept to other common error terms (e.g., mean absolute error). We evaluated our forecasts against an observation-based ensemble climatological forecast consisting of the observed monthly maximum daily streamflow values from the previous 20 years (e.g. Hauswirth et al., 2023), as well as EFAS seasonal hindcasts. We used the CRPSS to evaluate the probabilistic skill of our ML forecasts relative to the reference ensemble climatology. The CRPSS ranges between negative infinity and 1, where 1 indicates perfect skill and 0 or below indicates no skill compared to the reference forecast. We computed the CRPS of the forecast and reference for each month in the test period (2004-2016) and took the mean across individual months to compute the CRPSS.

We complemented the CRPS (CRPSS) with the anomaly correlation coefficient (ACC) and reliability index (RI) (Renard et al., 2010). The ACC varies between -1 and 1, with a score

of 1 representing perfect correlation between observed and forecast streamflow values. The RI is a probabilistic measure of the extent to which the forecast ensemble spread represents the uncertainty in observations. It varies between 0 and 1, with 1 denoting a perfectly reliable forecast. Like the CRPSS, we calculate the ACC and RI for every month and lead time separately. Lastly, we assessed the relative importance of the predictor variables using the Gini index, which measures the importance of individual variables in tree-based ML models. Specifically, the Gini index quantifies the extent to which a variable contributes to making homogeneous groups, where outcomes are similar and predictions are more reliable, while reducing impurity, indicating mixed groups with less predictable outcomes.

3 Results

The multi-site model with catchment attributes significantly outperforms the multi-site model with the catchment ID alone (Figure 2a). This suggests that including static catchment attributes enables the model to better reproduce the hydrologic behaviour of different catchments, aligning with previous research for the UK on ML applied to daily streamflow simulation using observed climate inputs (e.g. Lees et al., 2021; Lees et al., 2022), and with findings on the performance of ML models for prediction in ungauged basins (Kratzert et al. 2019). Considering the skill scores for each lead time and combining all initialization months, the multi-site model with catchment attributes narrowly but significantly outperforms the single-site models at lead times of one to three months, with a similar average performance between the multi-site and single-site model for the zeroth lead time (Figure 2b). However, the relative performance of the multi-site model with attributes and the single-site model varies by forecast month and lead time (Figure 3). For the zeroth lead time, the multi-site model tends to outperform the single-site model in the months where the highest skill is observed (i.e. December, January, June, July).

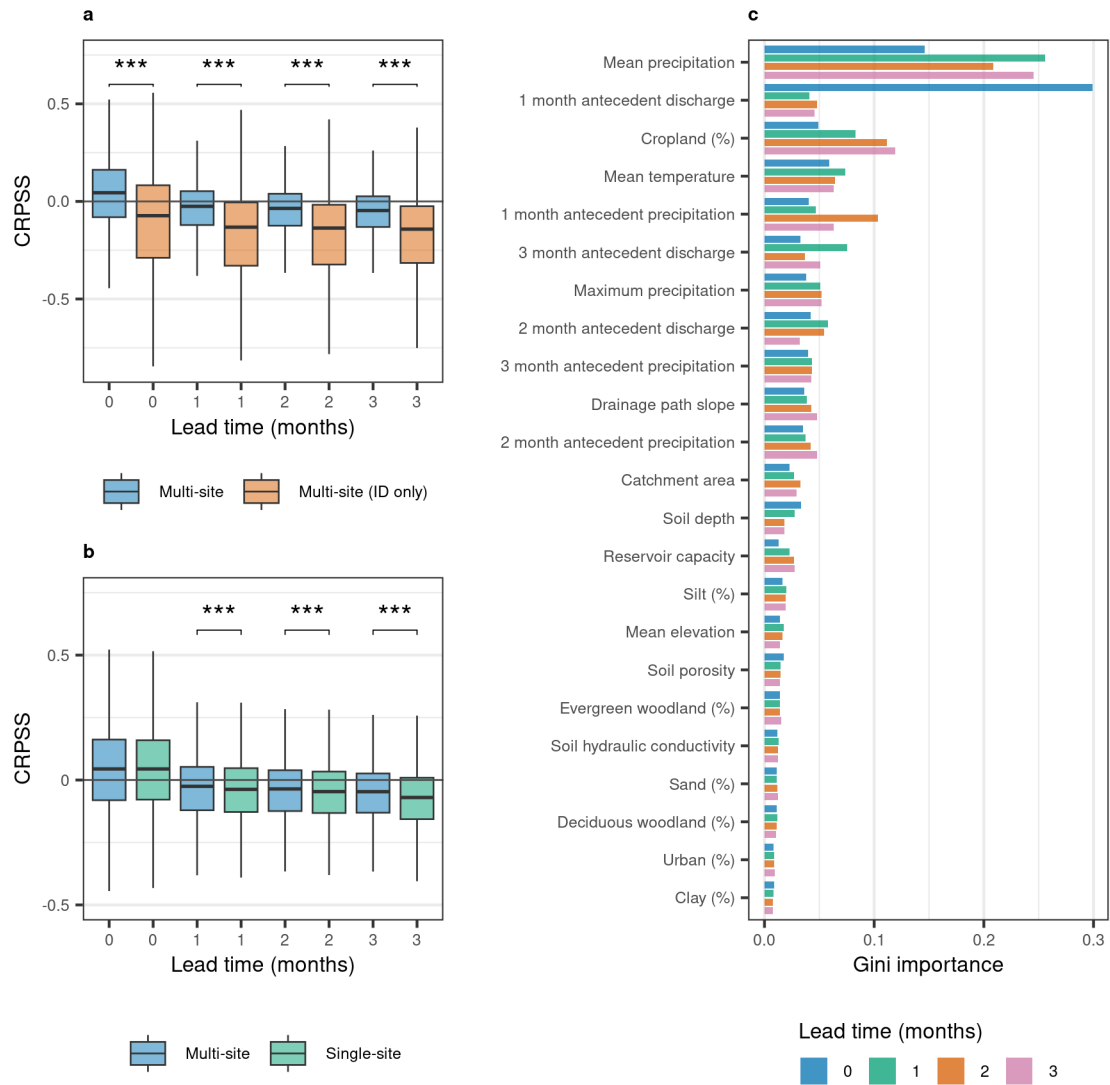


Figure 2: Analysis of model performance. **a.** Comparison of CRPSS for all months for multi-site models with catchment attributes and with the catchment ID only. We used a two-sided Wilcoxon signed rank test to assess whether differences in skill scores between the models were significant (***) = $p < 0.001$, ** = $p < 0.01$, * = $p < 0.05$). **b.** Comparison of single-site model with multi-site model with catchment attributes. **c.** Relative importance of predictor variables in the multi-site model with catchment attributes for each lead time. Time-varying predictors are marked with an asterisk (e.g. *Mean precipitation).

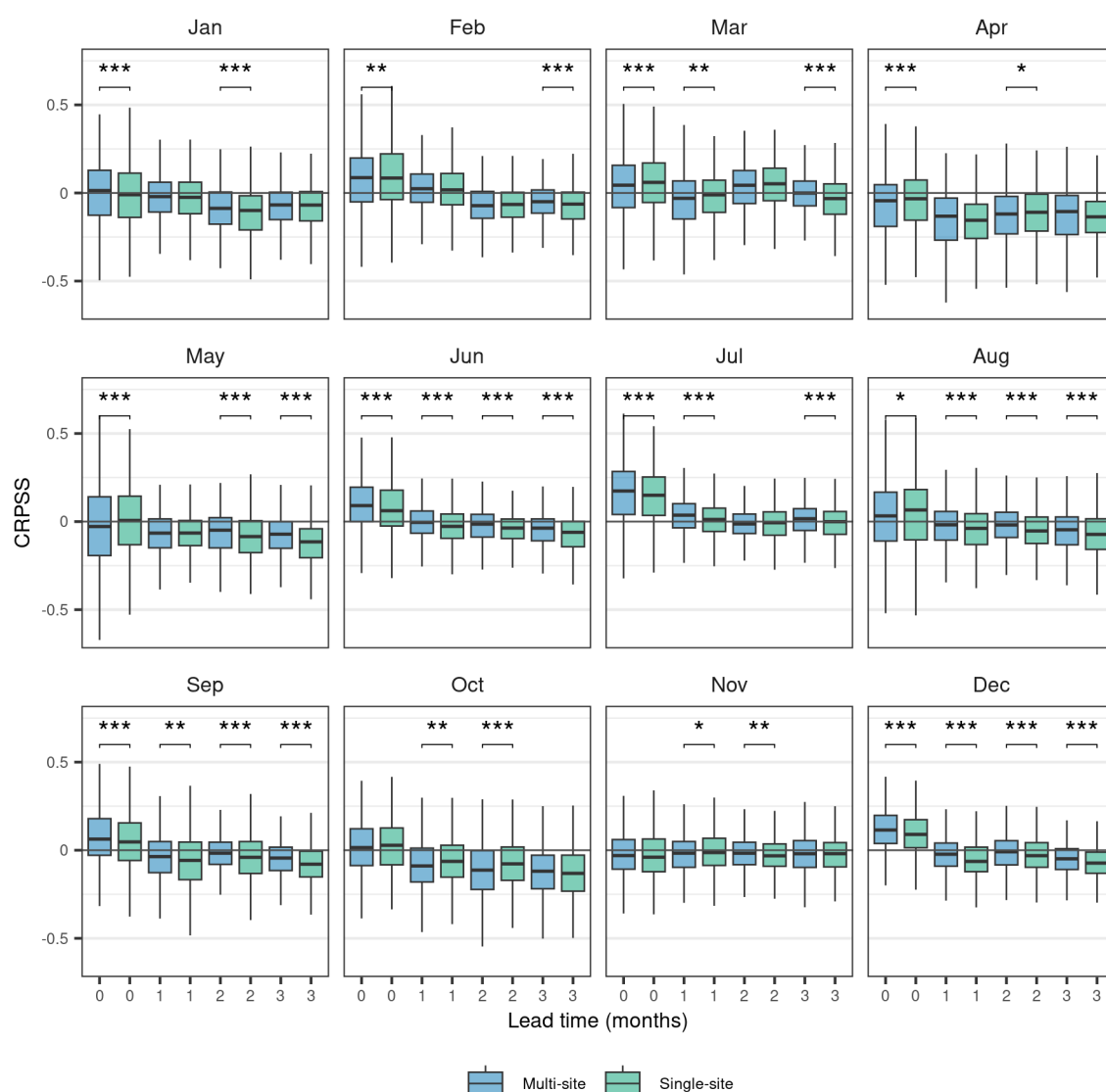


Figure 3: Comparison of CRPSS values for all forecast locations between the single-site model (green) and multi-site model with catchment attributes (blue) by month. The skill score uses a reference forecast of climatology. We used a one-sided Wilcoxon signed rank test to assess whether differences in skill scores between the models were significant (** = $p < 0.01$, * = $p < 0.05$).

We used the Gini index to assess the importance of each predictor variable to the multi-site model with catchment attributes at each lead time (Figure 2c). Monthly precipitation forecasts have high importance across lead times, while mean temperature forecasts have moderate importance. We also included antecedent conditions from observed streamflow and forecast precipitation. Antecedent streamflow is the most important variable at one-month lead time but decreases with importance at later lead

times. This is because we are limited to providing antecedent conditions prior to forecast initialization, which has decreasing relevance as the lead time increases, reflecting our general understanding of the influence of initial versus boundary conditions in S2S hydrologic forecasting (e.g. Wood et al., 2016).

We assessed skill by computing the monthly CRPSS using a climatological prediction as a reference. We find that there is significant variability in skill during the different months of the year (Figure 5a), especially at shorter lead times. For lead time 0, we observed the highest skill in extended winter (DJFM) and late summer (JJAS), with lower skill during spring and autumn. This is a positive result because in the UK high river flows are usually seen during the winter months. In December and July more than 80% of stations have positive skill in lead time 0 (Table 2). In most months, the skill decreases sharply over time, whereas for other months (e.g. March) the skill remains relatively consistent as lead time increases. The variation in skill likely reflects the varying importance of antecedent conditions during the year, as well as the varying skill of the climate forecasts.

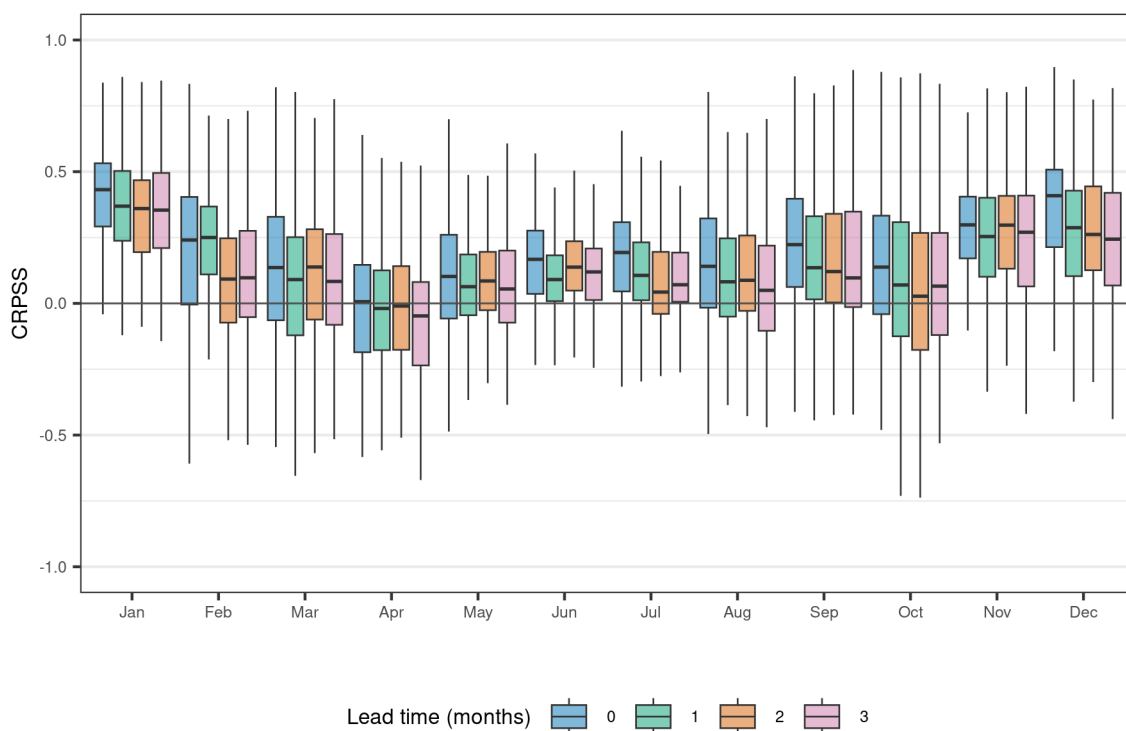


Figure 4: Continuous rank probability skill score of the multi-site model with catchment attributes using bias-corrected EFAS seasonal hindcasts as a benchmark.

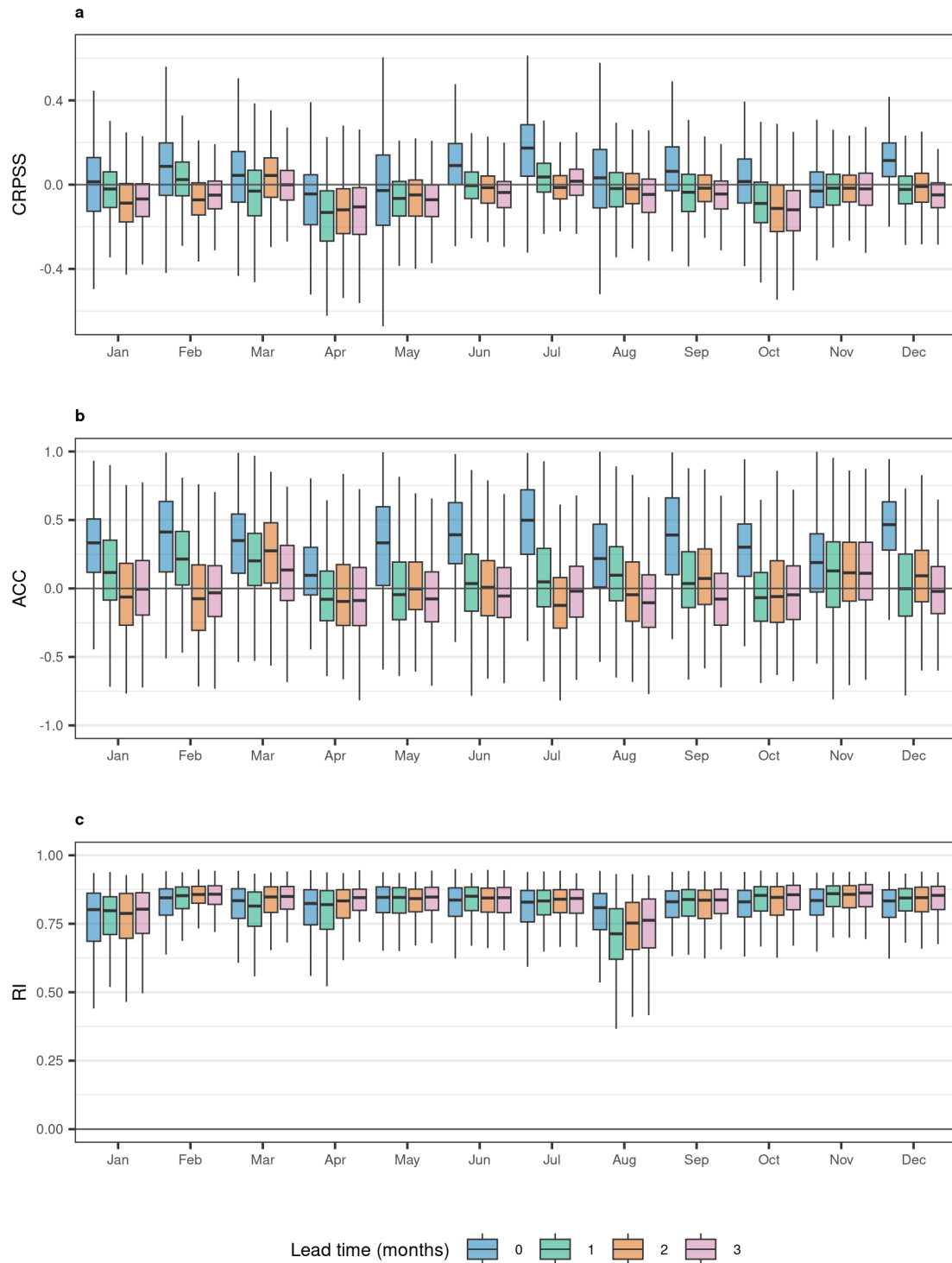


Figure 5: Performance assessment of the multi-site model with catchment attributes for each forecast month and lead time, using an ensemble climatological forecast as the reference. **a.** Continuous ranked probability skill score (CRPSS). We use climatological forecast as the reference forecast, which is computed separately for each test year in the

simulation. **b.** Anomaly correlation coefficient (ACC). **c.** Reliability index (RI). The four lead times are shown with different colours.

As with the CRPSS, the ACC varies by forecast month and lead time (Figure 5b), with the monthly variability in ACC following a similar pattern to that of the CRPSS. At lead time 0, the ACC is positive in >75% of stations across all months. During lead time 1, the ACC is positive in >50% of stations in all months except April, May, and October. Compared to the CRPSS and the ACC, the RI is more consistent across months and lead times (Figure 5c). Overall, our ensemble hindcasts have high reliability, with the mean RI across all stations exceeding 0.8 in all months except August.

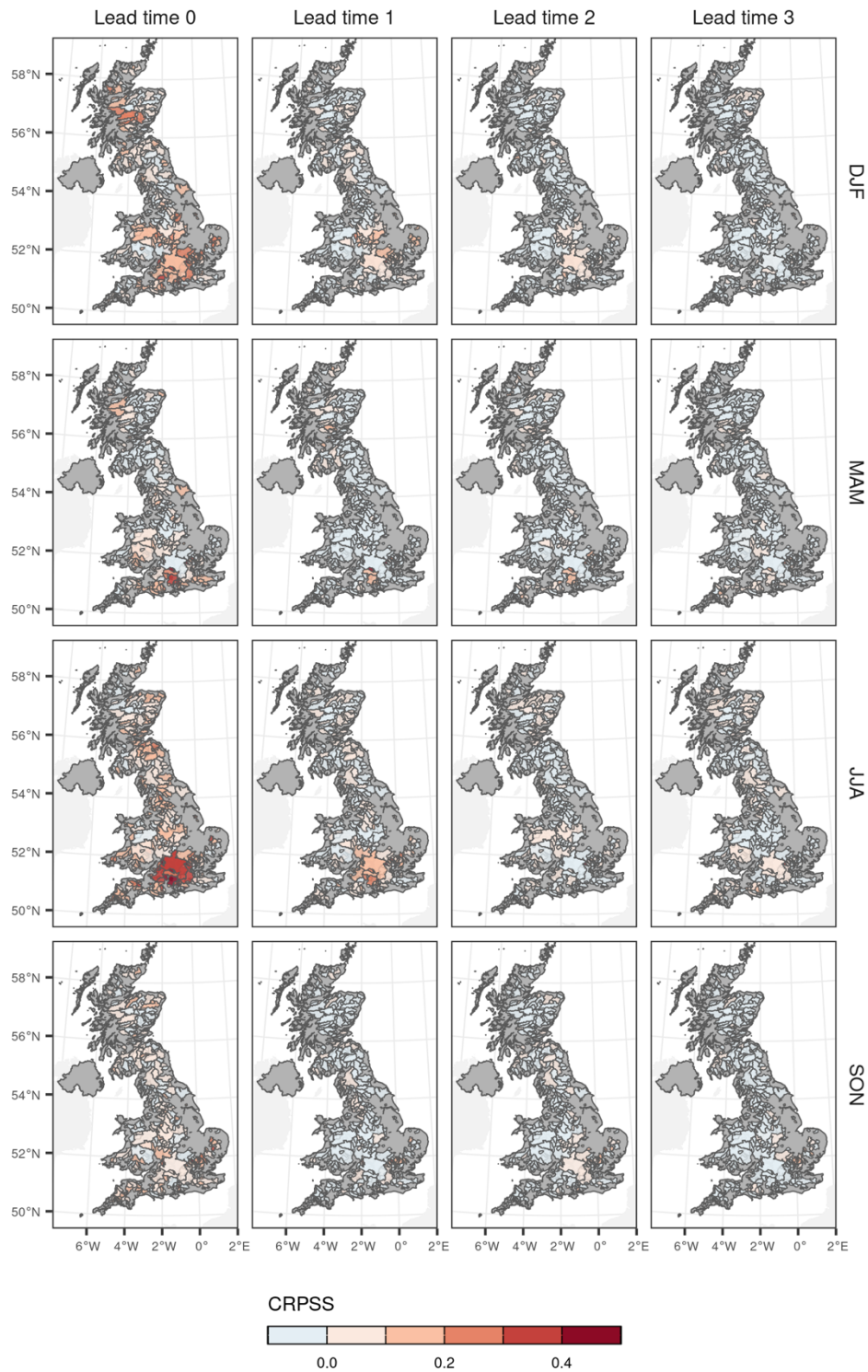
We also compared our results to monthly Q_{\max} drawn from daily EFAS seasonal predictions for a subset of the stations included in this study ($n=188$) that overlapped with the EFAS reference dataset. We bias corrected the EFAS outputs using a quantile mapping approach employing an empirical cumulative distribution function so that they could be directly compared with observations. As EFAS produces daily streamflow estimates we took the maximum daily streamflow prediction from each month and used this value as the reference forecast to estimate CRPSS. Our results are skilful compared to EFAS (Figure 4), and this high relative skill, coupled with the general lack of positive skill of the QRF forecast for lead times of 1-3 months compared to a climatological reference, indicates that the EFAS predictions were poorer than expected as a benchmark for this monthly extreme target variable. We note that our model is specifically trained to predict Q_{\max} , while EFAS seasonal forecasts are developed for more general purposes, such as supporting tercile probability forecasts for monthly or seasonal mean conditions, a common S2S hydrological product (e.g. Arnal et al., 2018).

Table 2: Percentage of stations ($n=579$) that are skilful ($\text{CRPSS}>0$) compared to climatological reference forecast at each lead time and forecast month for the multi-site model with catchment attributes.

Forecast month	Lead time			
	0	1	2	3
January	51.7	42.2	25.3	26.3
February	66.1	59.2	28.0	29.4

March	58.8	42.2	62.3	50
April	38.4	19.2	22.0	20.8
May	46.0	29.8	33.6	24.4
June	76.1	48.3	44.3	31.0
July	81.1	64.5	41.7	59.3
August	56.4	44.3	42.6	33.6
September	67.1	38.2	43.8	31.7
October	53.8	26.6	23.5	18.9
November	40.1	41.3	42.2	42.2
December	83.4	40.0	45.5	28.2

We examined the spatial variability in model skill by averaging the monthly skill scores for the multi-site model (with catchment attributes) within each season (Figure 6). At lead time 0 we observe skill across much of the UK, while at later lead times, skilful catchments tend to cluster in southern England. This could be related to the presence of relatively slower responding catchments with greater subsurface storage in the south-eastern UK. However, we found relatively weak correlation between ACC and the baseflow index ($R=0.33, 0.31, 0.27, 0.25$ for the four lead times). We observe a tendency for the QRF models to underestimate the observed Q_{\max} , especially the more extreme values (Figure 7). The underestimation is more pronounced as lead time increases, likely due to greater noise in the seasonal climate forecasts at longer lead times.



381

382 **Figure 6:** Average seasonal skill compared to climatological reference forecast in every
 383 catchment by lead time. We calculate the CRPSS per month and catchment, then compute
 384 the seasonal average (DJF, MAM, JJA, SON).

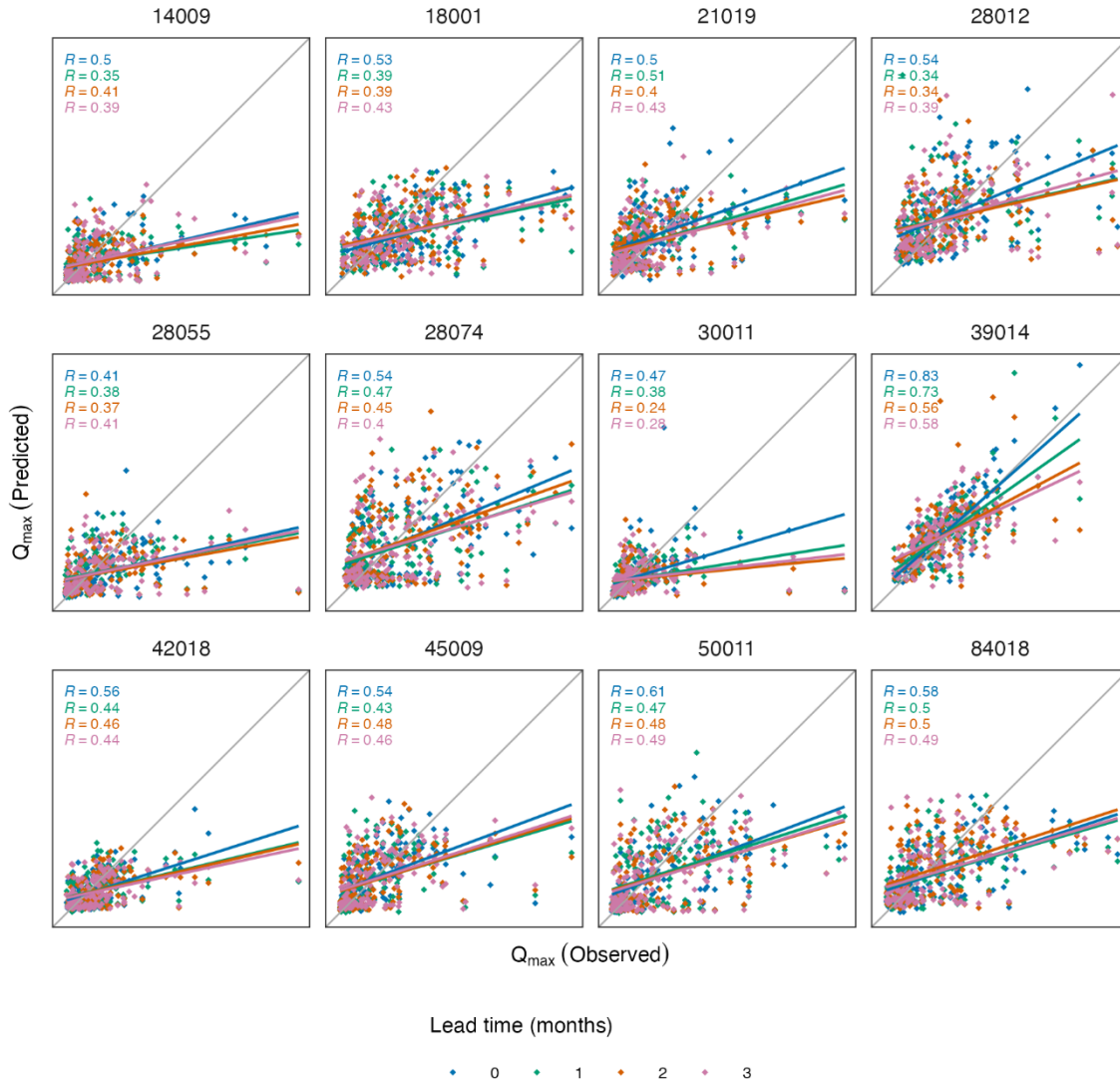


Figure 7: Comparison of observed and predicted Q_{\max} across all months for 12 randomly selected catchments, by lead time.

4 Discussion

We developed a hybrid forecasting approach for UK flood risk prediction at subseasonal-to-seasonal time scales using a large multimodel ensemble of climate predictions. Addressing our first research question, we found that S2S flood predictions are generally skilful (CRPSS>0) up to 1 month following initialization, but skill declines thereafter. However, 90 stations out of 579 retained positive skill in at least three months of the year for all four lead times. Across all initialization times, 60% of stations show positive skill compared to the climatological benchmark in the first month after initialization. This

proportion drops to 41% in the second month, 38% in the third month and 33% in the fourth month. The level of skill varies within the year, with some months generally more skilful than others. The seasonal variation in skill is likely due to a combination of varying climate predictability and the varying importance of antecedent conditions to flood magnitude and frequency during the year. The underlying seasonal forecasts of precipitation and temperature are also most skilful at shorter lead times, although they retain some information at longer lead times.

Our work provides guidance on how to build hybrid streamflow prediction systems that combine ML with dynamical model forecasts. With respect to our second research question, we found that a large-sample ML model trained on data from all catchments at once tends to outperform single-site model forecasts across all lead times. This results aligns with previous research on ML-based hydrological modelling, which revealed the benefit of a larger training dataset in large-sample models relative to single-site approaches (e.g. Kratzert et al., 2019). However, our work specifically considers forecasting months ahead, whereas previous work only studied out-of-sample simulation or short-term prediction using observed meteorological or weather forecast inputs. The large-sample approach enables ML models to combine information across time and space into a single model that is trained to discriminate a range of hydrological behaviours. The inclusion of static catchment attributes enables such models to learn the different rainfall-runoff behaviours across many catchments. This is especially important when using ML to predict extremes when training data are limited in time, as it means multi-site models remain realistic over a larger range of conditions than single-site models.

Hybrid prediction systems require training and testing partitions to evaluate model performance, and different approaches exist to do this. Here we implemented a forward-chain cross validation approach such that the model is never trained on data more recent than the test partition. This reproduces an operational setup as far as possible, where the model is never exposed to information from the future. However, one limitation of this approach for hindcast studies is that the relatively short hindcast period of the C3S multimodel ensemble (i.e. 1994-2016) means the smallest training partition may contain as few as 10 years of monthly data. Nevertheless, during model development we found that increasing the length of the training period – by focusing on the predictions from the SEAS5

system, which has an extended hindcast period of 1981-2016 – did not significantly enhance the performance of the QRF models (results not shown). Moreover, using a multi-site approach reduces the impact of the relatively short reforecast period by pooling data from many catchments to create a much larger training dataset than is used by single-site models (i.e. swapping space for time).

Our hybrid seasonal flood forecasts based on eight models from the C3S multimodel ensemble exhibit relatively low skill, as is also the case with traditional (i.e. process-based hydrological model) flood forecasting systems driven by C3S (e.g. Arnal et al., 2018). These findings suggest that the primary constraint on enhanced skill lies in the seasonal climate forecasts. Increasing the skill of climate forecasts is therefore a priority to achieve more useful seasonal streamflow forecasts. One area for further research is to develop ways of identifying ensemble members that are likely to be more skilful over a given time period. Selecting members based on their ability to reproduce large-scale climate patterns such as the NAO is one potential option that has proved successful in other applications (e.g. Dobrynin et al., 2022; Moulds et al., 2023). Observed climate states, teleconnections and indices (e.g., describing El Nino, the Southern Oscillation, and other climate modes) may be similarly exploited in regions where they exert an influence on weather patterns. These patterns have been deployed in empirical hydrologic forecast systems for many years, while the operational outputs from climate forecast models remain a relatively less-explored source of predictability in hybrid approaches.

5 Conclusion

Operational services for seasonal streamflow forecasts have existed for over a century, offering highly skilled predictions in many parts of the world, and particularly when and where predictors with long persistence are present – such as snowpack or groundwater – as well as strong climate seasonality. Despite their successes, there is growing demand from stakeholders for improved seasonal flow prediction skill at times and in places where it has been more difficult to achieve, usually due to data limitations or hydroclimate considerations.

This study illustrates that a hybrid multi-site forecasting approach trained over a large-sample collections of watersheds may offer benefits for monthly to seasonal predictions of streamflow. Our approach affords users significant flexibility to define target variables of interest (e.g. Q_{\max}). We use static catchment attributes as predictor variables to allow the QRF model to learn the different relationships between hydroclimate input data and monthly maximum daily streamflow, demonstrating an ability to produce skilful seasonal forecasts of monthly flood risk up to four months ahead in a moderate fraction of the catchments studied. The use of a multi-site ML model that is trained on data from multiple catchments at once may help to alleviate the long-standing problem of small sample sizes when training seasonal predictions on individual sites alone, while also enabling prediction in ungauged basins. However, although the performance benefit of the multi-site model over single-site models is statistically significant, the improvement is modest, suggesting that the primary constraint on enhancing skill remains the quality of seasonal climate forecasts themselves.

Competing interests

LJS is a member of the editorial board of HESS. The authors have no other competing interests to declare.

Acknowledgements

SM and LJS were supported by UKRI FLF grant MR/V022008/1. LJS was additionally supported by NERC grant NE/S015728/1. AW was supported by the United States Army Corps of Engineers Climate Preparedness and Resilience Program and AW and LA were also supported by the NOAA Cooperative Institute for Research to Operations in Hydrology (CIROH) through a Cooperative Agreement with The University of Alabama (NA22NWS4320003). The authors would like to acknowledge the use of the University of Oxford Advanced Research Computing (ARC) facility in carrying out this work (<http://dx.doi.org/10.5281/zenodo.22558>) and the UK National River Flow Archive (NRFA) for providing historical daily streamflow time series across Great Britain. We are grateful to Christel Prudhomme, Shaun Harrigan and Michel Wortmann at ECMWF for sharing the latest EFAS hindcasts.

484 **Data availability statement**

485 The input data and scripts that are needed to reproduce the results of this study will be
486 uploaded to a research data repository under an MIT license upon acceptance for
487 publication. They can be made available to reviewers upon request.

488 **References**

- 489 Arheimer, B., Pimentel, R., Isberg, K., Crochemore, L., Andersson, J. C. M., Hasan, A., &
490 Pineda, L. (2020). Global catchment modelling using World-Wide HYPE (WWH), open
491 data, and stepwise parameter estimation. *Hydrology and Earth System Sciences*,
492 24(2), 535–559. <https://doi.org/10.5194/hess-24-535-2020>
- 493 Arnal, L., Cloke, H. L., Stephens, E., Wetterhall, F., Prudhomme, C., Neumann, J., Krzeminski,
494 B., & Pappenberger, F. (2018). Skilful seasonal forecasts of streamflow over Europe?
495 *Hydrology and Earth System Sciences*, 22(4), 2057–2072.
496 <https://doi.org/10.5194/hess-22-2057-2018>
- 497 Bennett, J. C., Wang, Q. J., Robertson, D. E., Schepen, A., Li, M., & Michael, K. (2017).
498 Assessment of an ensemble seasonal streamflow forecasting system for Australia.
499 *Hydrology and Earth System Sciences*, 21(12), 6007–6030.
500 <https://doi.org/10.5194/hess-21-6007-2017>
- 501 Bierkens, M. F. P., & Van Beek, L. P. H. (2009). Seasonal Predictability of European
502 Discharge: NAO and Hydrological Response Time. *Journal of Hydrometeorology*,
503 10(4), 953–968. <https://doi.org/10.1175/2009JHM1034.1>
- 504 Breiman, L. (2001). Random forests. *Machine Learning*, 45(1), 5–32.
- 505 Coxon, G., Addor, N., Bloomfield, J. P., Freer, J., Fry, M., Hannaford, J., Howden, N. J. K.,
506 Lane, R., Lewis, M., Robinson, E. L., Wagener, T., & Woods, R. (2020). CAMELS-GB:
507 Hydrometeorological time series and landscape attributes for 671 catchments in

508 Great Britain. *Earth System Science Data*, 12(4), 2459–2483.

509 <https://doi.org/10.5194/essd-12-2459-2020>

510 Crochemore, L., Ramos, M.-H., & Pappenberger, F. (2016). Bias correcting precipitation
511 forecasts to improve the skill of seasonal streamflow forecasts. *Hydrology and Earth
512 System Sciences*, 20(9), 3601–3618. <https://doi.org/10.5194/hess-20-3601-2016>

513 Demargne, J., Wu, L., Regonda, S. K., Brown, J. D., Lee, H., He, M., Seo, D.-J., Hartman, R.,
514 Herr, H. D., Fresch, M., Schaake, J., & Zhu, Y. (2014). The Science of NOAA’s
515 Operational Hydrologic Ensemble Forecast Service. *Bulletin of the American
516 Meteorological Society*, 95(1), 79–98. <https://doi.org/10.1175/BAMS-D-12-00081.1>

517 Doblas-Reyes, F. J., García-Serrano, J., Lienert, F., Biescas, A. P., & Rodrigues, L. R. L. (2013).
518 Seasonal climate predictability and forecasting: Status and prospects. *WIREs Climate
519 Change*, 4(4), 245–268. <https://doi.org/10.1002/wcc.217>

520 Dobrynin, M., Düsterhus, A., Fröhlich, K., Athanasiadis, P., Ruggieri, P., Müller, W. A., &
521 Baehr, J. (2022). Hidden Potential in Predicting Wintertime Temperature Anomalies
522 in the Northern Hemisphere. *Geophysical Research Letters*, 49(20).
523 <https://doi.org/10.1029/2021GL095063>

524 Emerton, R., Zsoter, E., Arnal, L., Cloke, H. L., Muraro, D., Prudhomme, C., Stephens, E. M.,
525 Salamon, P., & Pappenberger, F. (2018). Developing a global operational seasonal
526 hydro-meteorological forecasting system: GloFAS-Seasonal v1.0. *Geoscientific Model
527 Development*, 11(8), 3327–3346. <https://doi.org/10.5194/gmd-11-3327-2018>

528 Gauch, M., Mai, J., & Lin, J. (2021). The proper care and feeding of CAMELS: How limited
529 training data affects streamflow prediction. *Environmental Modelling & Software*,
530 135, 104926. <https://doi.org/10.1016/j.envsoft.2020.104926>

531 Harrigan, S., Prudhomme, C., Parry, S., Smith, K., & Tanguy, M. (2018). Benchmarking
 532 ensemble streamflow prediction skill in the UK. *Hydrology and Earth System*
 533 *Sciences*, 22(3), 2023–2039. <https://doi.org/10.5194/hess-22-2023-2018>
 534 Hauswirth, S. M., Bierkens, M. F. P., Beijk, V., & Wanders, N. (2023). The suitability of a
 535 seasonal ensemble hybrid framework including data-driven approaches for
 536 hydrological forecasting. *Hydrology and Earth System Sciences*, 27(2), 501–517.
 537 <https://doi.org/10.5194/hess-27-501-2023>
 538 Kratzert, F., Klotz, D., Herrnegger, M., Sampson, A. K., Hochreiter, S., & Nearing, G. S. (2019).
 539 Toward Improved Predictions in Ungauged Basins: Exploiting the Power of Machine
 540 Learning. *Water Resources Research*, 55(12), 11344–11354.
 541 <https://doi.org/10.1029/2019WR026065>
 542 Lees, T., Buechel, M., Anderson, B., Slater, L., Reece, S., Coxon, G., & Dadson, S. J. (2021).
 543 Benchmarking data-driven rainfall–runoff models in Great Britain: A comparison of
 544 long short-term memory (LSTM)-based models with four lumped conceptual models.
 545 *Hydrology and Earth System Sciences*, 25(10), 5517–5534.
 546 <https://doi.org/10.5194/hess-25-5517-2021>
 547 Lehner, F., Wood, A. W., Llewellyn, D., Blatchford, D. B., Goodbody, A. G., & Pappenberger,
 548 F. (2017). Mitigating the Impacts of Climate Nonstationarity on Seasonal Streamflow
 549 Predictability in the U.S. Southwest. *Geophysical Research Letters*, 44(24).
 550 <https://doi.org/10.1002/2017GL076043>
 551 Meinshausen, N. (2006). Quantile Regression Forests. *Journal of Machine Learning Research*,
 552 7, 983–999.
 553 Mendoza, P. A., Wood, A. W., Clark, E., Rothwell, E., Clark, M. P., Nijssen, B., Brekke, L. D., &
 554 Arnold, J. R. (2017). An intercomparison of approaches for improving operational

555 seasonal streamflow forecasts. *Hydrology and Earth System Sciences*, 21(7), 3915–
556 3935. <https://doi.org/10.5194/hess-21-3915-2017>

557 Moulds, S., Slater, L. J., Dunstone, N. J., & Smith, D. M. (2023). Skillful Decadal Flood
558 Prediction. *Geophysical Research Letters*, 50(3), e2022GL100650.
559 <https://doi.org/10.1029/2022GL100650>

560 Nearing, G. S., Kratzert, F., Sampson, A. K., Pelissier, C. S., Klotz, D., Frame, J. M., Prieto, C., &
561 Gupta, H. V. (2021). What Role Does Hydrological Science Play in the Age of Machine
562 Learning? *Water Resources Research*, 57(3), e2020WR028091.
563 <https://doi.org/10.1029/2020WR028091>

564 Regonda, S. K., Rajagopalan, B., & Clark, M. (2006). A new method to produce categorical
565 streamflow forecasts. *Water Resources Research*, 42(9), 2006WR004984.
566 <https://doi.org/10.1029/2006WR004984>

567 Renard, B., Kavetski, D., Kuczera, G., Thyer, M., & Franks, S. W. (2010). Understanding
568 predictive uncertainty in hydrologic modeling: The challenge of identifying input and
569 structural errors. *Water Resources Research*, 46(5), 2009WR008328.
570 <https://doi.org/10.1029/2009WR008328>

571 Slater, L. J., Arnal, L., Boucher, M.-A., Chang, A. Y.-Y., Moulds, S., Murphy, C., Nearing, G.,
572 Shalev, G., Shen, C., Speight, L., Villarini, G., Wilby, R. L., Wood, A., & Zappa, M.
573 (2023). Hybrid forecasting: Blending climate predictions with AI models. *Hydrology
574 and Earth System Sciences*, 27(9), 1865–1889. [https://doi.org/10.5194/hess-27-](https://doi.org/10.5194/hess-27-1865-2023)
575 1865-2023

576 Tian, D., He, X., Srivastava, P., & Kalin, L. (2022). A hybrid framework for forecasting monthly
577 reservoir inflow based on machine learning techniques with dynamic climate
578 forecasts, satellite-based data, and climate phenomenon information. *Stochastic*

579 *Environmental Research and Risk Assessment*, 36(8), 2353–2375.

580 <https://doi.org/10.1007/s00477-021-02023-y>

581 Tyrallis, H., Papacharalampous, G., & Langousis, A. (2019). A Brief Review of Random Forests

582 for Water Scientists and Practitioners and Their Recent History in Water Resources.

583 *Water*, 11(5), 910. <https://doi.org/10.3390/w11050910>

584 Wilks, D. S. (2019). Forecast Verification. In *Statistical Methods in the Atmospheric Sciences*

585 (pp. 369–483). Elsevier. <https://doi.org/10.1016/B978-0-12-815823-4.00009-2>

586 Wood, A. W., Hopson, T., Newman, A., Brekke, L., Arnold, J., & Clark, M. (2016). Quantifying

587 Streamflow Forecast Skill Elasticity to Initial Condition and Climate Prediction Skill.

588 *Journal of Hydrometeorology*, 17(2), 651–668. [https://doi.org/10.1175/JHM-D-14-](https://doi.org/10.1175/JHM-D-14-0213.1)

589 0213.1

590 Yuan, X., Wood, E. F., & Ma, Z. (2015). A review on climate-model-based seasonal hydrologic

591 forecasting: Physical understanding and system development. *WIREs Water*, 2(5),

592 523–536. <https://doi.org/10.1002/wat2.1088>

593